Hindawi
Advances in Civil Engineering
Volume 2021, Article ID 9915947, 14 pages
https://doi.org/10.1155/2021/9915947

Research Article

Construction Stage Seismic Vulnerability Evaluation of a Continuous Girder Bridge with the Cast-in-Place Cantilever Construction Method

Hongxu Li,[1,2] **Yong Huang**,[1,2] **and Endong Guo**[1,2]

[1]*Institute of Engineering Mechanics, China Earthquake Administration, Harbin 150080, China*
[2]*Key Laboratory of Earthquake Engineering and Engineering Vibration of China Earthquake Administration, Harbin 150080, China*

Correspondence should be addressed to Yong Huang; huangyong@iem.ac.cn

Received 1 April 2021; Revised 13 August 2021; Accepted 25 August 2021; Published 3 September 2021

Academic Editor: Sonia E. Ruiz

To evaluate the vulnerability of bridges at various construction stages under the action of strong earthquakes, the incremental dynamic analysis (IDA) method is applied, and the vulnerabilities of a continuous girder case study bridge with the cast-in-place cantilever construction method, which owns five main construction stages, are evaluated and compared. The results show the following: With the increase in the peak ground acceleration (PGA), the vulnerabilities of bridges at different construction stages all increase. The fragility and vulnerability are mainly determined by the structural mechanical system condition and the mode shapes but not the modal frequency. For the working condition of seismic PGA of 0.4 g, (1) the bridge at the substructure construction stage may only experience slight or moderate damage with the exceedance probability of 8% to 5% and the mean loss ratio being only about 5%; (2) the vulnerabilities of bridges at the middle cantilever construction stage and the long cantilever construction stage are similar, the collapse damage exceedance probability is about 80%, and the mean loss ratio is about 65%; and (3) the vulnerabilities of bridges at the middle span closure construction stage and the bridge completion construction stage are nearly the same, the collapse damage exceedance probability is about 98%, and the mean loss ratio can reach 80%. The research results explore a new method for evaluating the vulnerability of bridges at different construction stages, which can provide suggestions for seismic damage defense and seismic insurance risk evaluation.

1. Introduction

In the statistics [1] of 279 bridge collapse cases after the year of 2000, the bridges with construction collapse cases comprised 46.59%, whereas natural disasters accounted for 28.32%. It is obvious that construction and natural disasters are important risk factors leading to bridge collapse accidents. Therefore, if a bridge under construction experiences an earthquake, the safety of the bridge will be seriously threatened. It is of great theoretical and practical significance to evaluate the antiseismic capacity of buildings [2]. Great attention should be paid to the seismic vulnerability evaluation, especially for bridges under construction.

For the study of the seismic vulnerability of bridges, most of the research studies have been conducted on completed bridges [3, 4]. To study the seismic fragility of long-span suspension bridges, Lu et al. [5] applied the probabilistic seismic demand models (PSDMs) method and improved a design based on fragility. Wu et al. [6] applied the incremental dynamic analysis (IDA) method and obtained the seismic capacity residual ratio of a structure. Zhang and Huo [7] used the frequency analysis method of exceeding the limit state along with the IDA method to analyze the seismic isolated bridge. Pan et al. [8] proposed a curve fitting method based on the damage index demand to capability ratio model to analyze the seismic vulnerability of New York continuous steel bridges. Cao et al. [9] studied the seismic fragility of multispan continuous girder bridges with consideration of the bond-slip behavior using the IDA method. Relatively little research has been done on the seismic vulnerability of

bridges during construction. In 2016, Yang et al. [10] analyzed the vulnerability of the whole process of the cantilever method for the concrete-filled steel tube superposed pier of a high-pier bridge in a mountainous area to analyze the risk of aftershock damage during the reconstruction of the bridge in an earthquake zone. Ohashi and Kiyomiya [11] performed a seismic safety analysis of a cable-stayed bridge with the suspension method, which included five construction stages. Hsu et al. [12] proposed a construction classification and vulnerability evaluation framework for different construction stages for Taiwan's buildings in 2013.

From the point of view of earthquake insurance, the existing commercial catastrophe risk models assume that a completed bridge has invariable vulnerability. However, this is not suitable for construction process risk because the vulnerabilities of bridges at every construction stage are different and these vulnerabilities may be more or less than those of a completed bridge. To evaluate the seismic risk of bridges under construction, it is important to research the differences of the seismic vulnerabilities of bridges at different construction stages.

In this research, a prestressed concrete continuous girder bridge with the cantilever method will be taken as the example to research the construction stage seismic vulnerability evaluation method. With consideration of the mechanical characteristics at different construction stages, five construction stages, which include the substructure, middle cantilever, long cantilever, middle span closure, and bridge completion stages, are comparatively researched on their seismic vulnerabilities. The seismic vulnerabilities of the bridges at different construction stages are evaluated by utilizing the IDA method.

2. Seismic Vulnerability Evaluation Method for Construction Stages

In this study, the fragility means the probability of structural response to exceed critical states under some seismic intensity measure. The vulnerability means the structural mean loss ratio under some seismic intensity measure. The fragility measures probability and vulnerability measure loss [13]. Therefore, the vulnerability evaluation is the computation process of the structural mean loss ratio.

In this study, the vulnerability evaluation method is as follows:

(1) Based on the practical construction method of the researched bridge, the whole construction process should be divided into different construction stages by considering different mechanical characteristics.

(2) The finite element modeling (FEM) of the bridge model should be developed by considering different construction stages. The incremental dynamic analysis method is applied to calculate the seismic demand values at different construction stages and for a range of earthquake intensities.

(3) For the bridge vulnerability evaluation under the action of strong earthquakes, the pier bottom sections are always regarded as fragile units. The moment-curvature values of the pier bottom sections are always regarded as the antiseismic capacity. The antiseismic capacity values can be obtained according to section characteristics, such as section size, material performance, and rebar layout.

(4) The ratios of the seismic demand value to the antiseismic capacity value at different construction stages and for different earthquake intensities can be calculated. In the log-log coordinate system, the function is fitted with the logarithm of the seismic intensity measure as the independent variable and the logarithm of the seismic demand value for the antiseismic capacity value ratio as the dependent variable.

(5) The longitudinal and transversal fragilities should be separately calculated. The seismic fragility curves of the bridge with comprehensive consideration of the longitudinal and transversal fragilities can be achieved.

(6) The loss ratios at different damage states are found based on reference [14]. The mean loss ratios at different construction stages are calculated for different peak ground accelerations (PGAs). The seismic mean loss ratios of the bridges at different construction stages can then be determined.

The flow chart of the vulnerability evaluation method is shown in Figure 1. In Figure 1, the information in the double boxes is the basic data that should be collected before the vulnerability evaluation, while the information in the single boxes is the intermediate variable in the evaluation process.

Figure 1 shows that the antiseismic capacity, seismic demand, fragility, and mean loss ratio are the core elements in the seismic vulnerability evaluation process, and they are the key factors for determining the structural seismic vulnerability.

3. Case Study Bridge Finite Element Modeling

3.1. Case Study Bridge Introduction. In this study, a prestressed concrete continuous girder bridge with the cast-in-place cantilever construction method is selected as a case study bridge to research the bridge vulnerability characteristics in the construction process.

The case study bridge has three spans. The first, second, and third spans are 51 m, 85 m, and 51 m, respectively. The girder cross section is a single box variable section. The elevation view of the middle span girder is shown in Figure 2.

The height of the pier is 9 m. All of the pier cross sections are rectangle sections with a size of 3.5 m × 7 m. The reinforcement layout of the pier bottom section is shown in Figure 3.

The bridge girder applies the cast-in-place cantilever construction method. The main construction stages are as follows: (1) substructure construction stage, (2) girder cantilever with blocks construction stages, (3) the 1st and 3rd span cast-in-place construction stages, (4) the 1st and 3rd span closure construction stages, (5) the middle span closure construction stage, and (6) the bridge completion stage. The

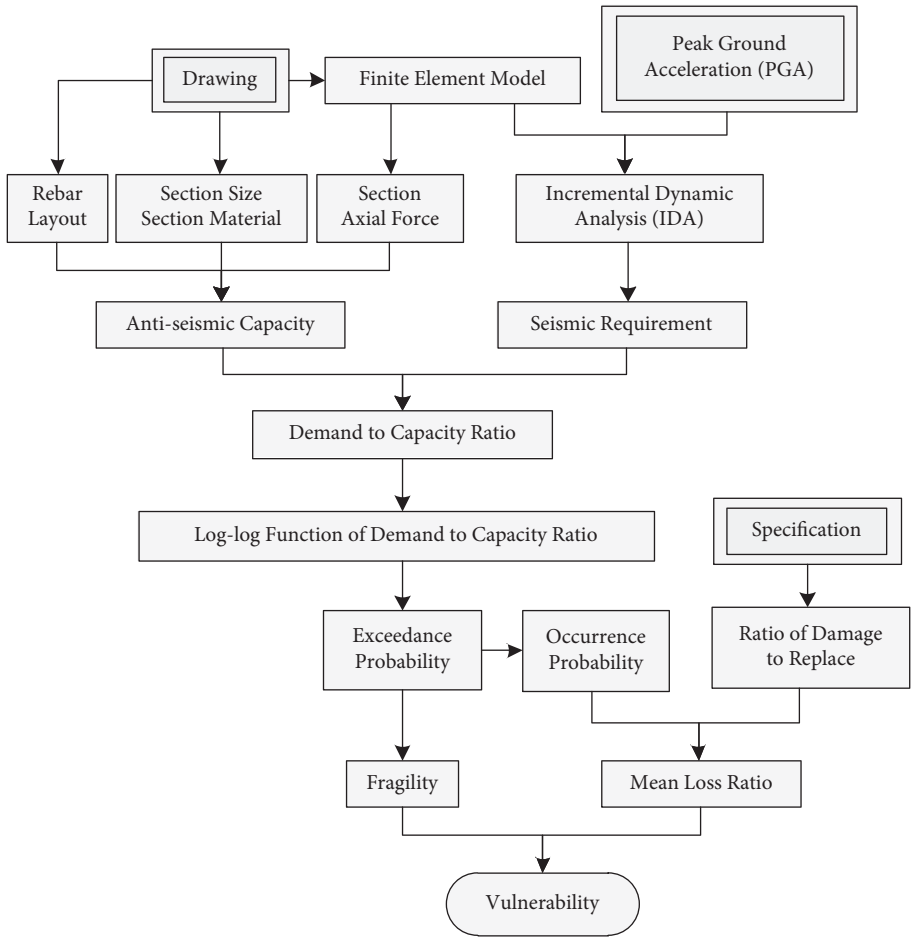

Figure 1: Flow chart of the vulnerability evaluation method.

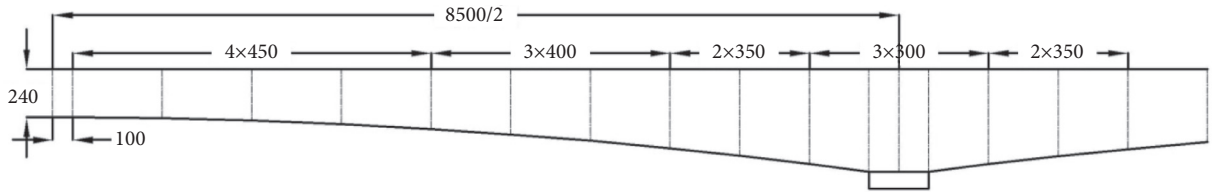

Figure 2: Elevation view of the middle span girder (dimension units: cm).

girder cantilever with blocks construction stages include the hanging basket, cast, prestress tension, and the other construction substages.

In reference to the practical seismic damage characteristics of the cast-in-place cantilever construction method, based on the case study bridge practical construction organization scheme, the seismic vulnerability of five typical construction stages are selected as the research object in this paper. The comparatively researched construction stages are listed in Table 1.

3.2. Finite Element Modeling. For this study, the finite element model of the bridge is developed using the software Midas Civil. The cushion caps, piers, and girders are modeled by beam elements, and their materials are C35 concrete, C40 concrete, and C60 concrete, respectively. The prestress steels in the girders are high strength low relaxation strands with a standard strength of 1860 MPa, and the posttensioned construction method is applied. The supports are simulated by elastic coupling. The soil-structure interaction is ignored. The Construction Stages function in the Midas Civil is applied to simulate the bridges at different construction stages by activating or killing the relevant element, boundary, and loads. The researched construction stages in this study are shown in Figure 4. The boundary condition is that the bridge is fixed at the bottoms of the cushion caps, which is shown as green points in Figure 4.

The modal information of the FEM for all the considered stages is listed in Table 2.

Twenty seismic records from five practical earthquakes that occurred in eastern China are selected as the seismic

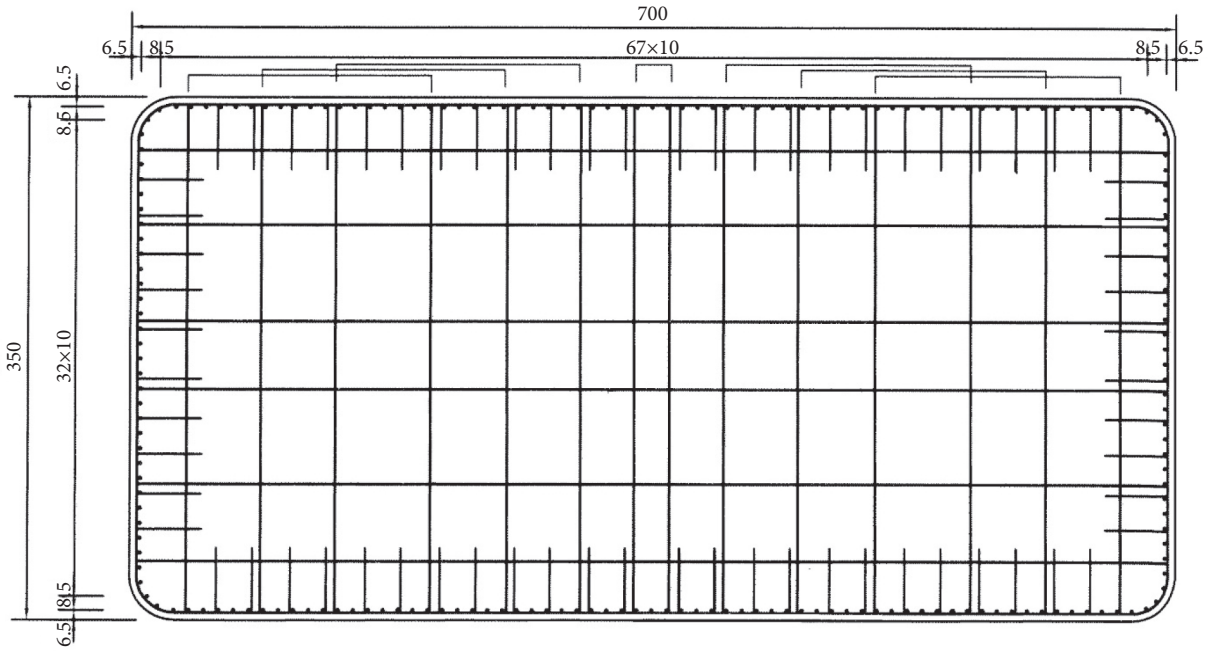

Figure 3: Reinforcement layout of the pier bottom section (dimension units: cm).

Table 1: Comparatively researched construction stages.

No.	Researched construction stage
1	Substructure
2	Middle cantilever
3	Long cantilever
4	Middle span closure
5	Bridge completion

excitation in the FEM software. Each of the records contains three record components, which are assumed to be oriented along the transversal, longitudinal, and vertical directions of the bridge. The identification of the considered seismic records is listed in Table 3. The seismic records data for this study are provided by Institute of Engineering Mechanics, China Earthquake Administration.

With regard to the relationship between the ground motion acceleration and the seismic fortification intensity [15–17], as well as for the structural probable damage situation, the PGAs are modified to 0.1 g, 0.2 g, 0.4 g, 0.8 g, and 1.0 g. The seismic response spectra of the seismic records are shown in Figure 5. The damping ratio used to develop the response spectra is 5%, and the response spectra are drawn from the twenty seismic records.

4. Case Study Bridge Seismic Vulnerability Evaluation

4.1. Antiseismic Capacity Analysis. To analyze the middle pier bottom section mechanical performance, some key parameters, such as the section shape, section size, concrete, rebar, rebar layout (as shown in Figure 3), and loading, are considered. The nominal moment-curvature [18] (which is called the computational curve in this paper) and the fitted double-linear moment-curvature (which is called idealized curve in this paper) relationships of the middle pier bottom section can be determined. Based on references [16, 19, 20], the first yield point, effective yield point, and ultimate point can be got. Then the first yield point and effective yield point can be connected into a line, and the line can be extended to the initial point; similarly, the effective yield point and ultimate point can be connected into a line. The above-mentioned two lines constitute the idealized curve. The middle pier bottom section moment-curvature relationships of the bridge completion stage are taken as the example, as shown in Figure 6.

The moment-curvature idealized relationship of the pier bottom sections is used to control the nonlinear behavior by the form of plastic hinges in the Midas Civil. The moment and curvature of the pier bottom sections will change along the idealized curve in Figure 6.

Based on reference [8], the first yield point, the effective yield point, the maximum moment point, and the ultimate point are selected as the damage boundary values in the seismic fragility evaluation process. The middle pier bottom section damage boundary values of the bridge completion stage are taken as the example and shown in Figure 6; the detail values are listed in Table 4.

4.2. Seismic Demand Analysis. In the seismic demand analysis process, the IDA method is applied. For the twenty seismic records, the PGAs are modified to 0.1 g, 0.2 g, 0.4 g, 0.8 g, and 1.0 g as the seismic excitation. So, there are 100 seismic load working conditions in total for every construction stage. After the finite element nonlinear time-history analysis in the Midas Civil, the transversal and longitudinal maximum moments of the middle pier bottom can be achieved. The IDA results of the middle pier bottom

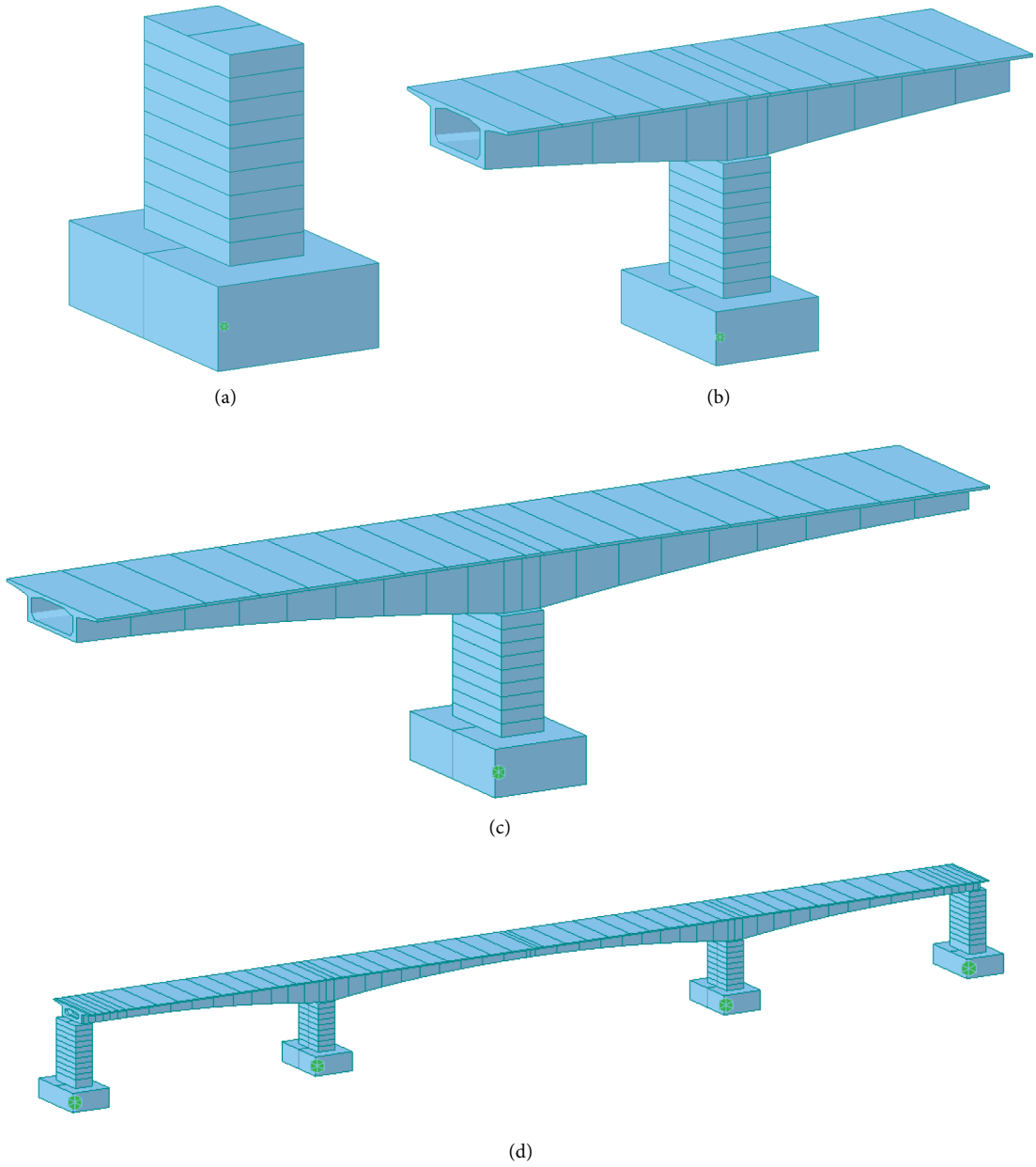

Figure 4: Researched construction stages for the case study bridge. (a) Substructure construction stage. (b) Middle cantilever construction stage. (c) Long cantilever construction stage. (d) Middle span closure construction stage and bridge completion construction stage.

at the bridge completion stage for twenty seismic excitations are taken as the example, as listed in Table 5.

Table 5 shows that for the case study bridge middle pier bottom, the transversal maximum moments are always larger than the longitudinal maximum moments. This may result in the transversal direction being more vulnerable than the longitudinal direction for the case study bridge.

4.3. Seismic Fragility Analysis. Based on the damage index demand for the capacity ratio method, the bridge seismic fragility situations at different construction stages are analyzed in this study. For each damage state, the natural logarithm of the input PGA to the 1 g ratio ($\ln(\mathrm{PGA})$) is regarded as the abscissa, and the natural logarithm of the demand to capacity ratio ($\ln(S_d/S_c)$) is regarded as the ordinate. Then, the log-log plot can be achieved. With the least square method, the linear functions can be fitted as shown in

$$\ln\left(\frac{S_d}{S_c}\right) = A * \ln(\mathrm{PGA}) + B, \tag{1}$$

where PGA is the ratio of the input PGA to 1 g; S_d is the seismic demand, which is the seismic response curvature of the middle pier bottom in this article (1/m); S_c is the

Table 2: The modal information of the FEM.

Construction stage	Modal no.	Frequency (Hz)	Mode shape	Mode shape description
Substructure	1	21.236	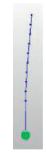	Middle pier longitudinal bends
	2	34.176		Middle pier transversal bends
	3	81.022		Middle pier longitudinal bends
Middle cantilever	1	2.378	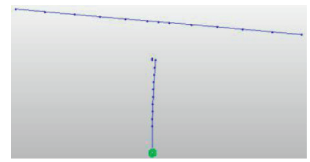	Middle pier longitudinal bends; main girder rotates around the supporter transversal direction
	2	3.539	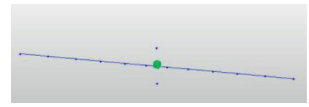	Main girder rotates around the supporter vertical direction
	3	5.932	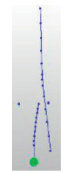	Middle pier transversal bends; main girder transversal bends
Long cantilever	1	1.161	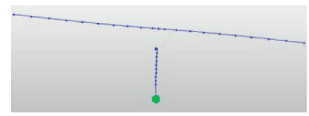	Pier longitudinal bends; main girder rotates around the supporter transversal direction
	2	1.458	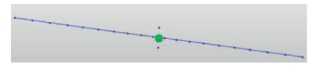	Main girder rotates around the supporter vertical direction
	3	2.570	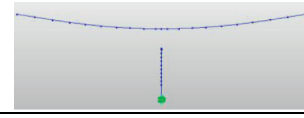	Main girder vertical bends
Middle span closure/ bridge completion	1	1.359		Main girder vertical bends
	2	2.421	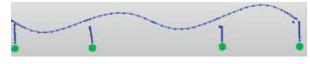	One middle pier transversal bends; main girder vertical bends
	3	3.128		Middle piers transversal bends; main girder transversal bends

antiseismic capacity, which is the damage boundary curvature of the middle pier bottom in this article (1/m); S_d/S_c is the ratio of demand to capacity; and A and B are the coefficients in the linear function. The coefficients and standard deviations (SD) in the linear function fitting process are listed in Table 6.

Table 3: Identification of the considered seismic records.

Time (UTC + 8)	Epicenter position	Magnitude (Ms)	Depth (km)	Station position	Site condition
2011-01-19 12 : 07 : 43	N30.659, E117.099	4.4	6	N32.000, E119.199	Soil
				N31.700, E119.000	Soil
				N31.500, E119.300	Soil
				N31.600, E118.300	Soil
				N31.500, E118.300	Soil
2012-07-20 20 : 11 : 51	N33.04, E119.569	4.9	15	N34.400, E118.400	Soil
				N33.299, E119.300	Soil
				N32.799, E120.300	Soil
				N32.099, E119.699	Soil
				N33.799, E119.800	Soil
2013-11-23 13 : 44 : 11	N37.099, E120.019	4.5	10	N36.799, E118.900	Soil
				N36.400, E119.800	Soil
				N36.500, E119.400	Soil
				N36.799, E119.800	Rock
				N37.599, E121.000	Rock
2014-03-19 20 : 19 : 22	N24.049, E122.419	5.9	10	N26.600, E118.199	Rock
				N25.500, E119.800	Rock
				N25.700, E117.099	Rock
2014-05-21 08 : 21 : 13	N23.76, E121.489	5.9	20	N25.799, E116.400	Rock
				N25.500, E119.800	Rock

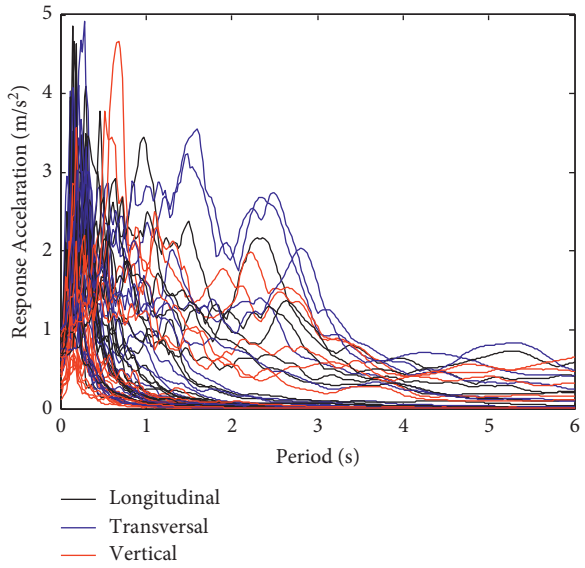

Figure 5: Seismic response spectra of the twenty seismic records.

The most common form of a seismic fragility function is the lognormal cumulative distribution function (CDF) [13]. The exceedance probability of $S_d/S_c > 1$ is

$$P_f = P\left(\frac{S_d}{S_c} > 1\right) = P\left[\ln\left(\frac{S_d}{S_c}\right) > \ln 1\right] = 1 - \Phi\left(\frac{\ln 1 - \mu}{\sigma}\right) = \Phi\left(\frac{\mu}{\sigma}\right), \quad (2)$$

where the mean value of the natural logarithm of the demand to capacity ratio is

$$\mu = \ln\left(\frac{S_d}{S_c}\right). \quad (3)$$

Additionally, the standard deviation of the natural logarithm of the demand to the capacity ratio is

$$\sigma = \sqrt{\frac{S_r}{n-2}}, \quad (4)$$

where S_r is the variance of natural logarithm of the demand to capacity ratio; n is the sample size of the natural logarithm of the demand to capacity ratio.

Based on equations (2)–(4), all the longitudinal and transversal exceedance probabilities of different damage states at different construction stages for different PGAs can be computed. Then, the seismic fragility of the bridge after comprehensive consideration of the longitudinal and transversal fragility curves can be determined. These curves are shown in Figure 7.

Figure 7 shows that for the substructure construction stage with a PGA of 0.4 g, the exceedance probabilities of the slight, moderate, extensive, and collapse damage states are about 8%, 5%, 0%, and 0%, respectively. This means, under the action of strong earthquakes, a bridge at the substructure construction stage hardly suffers from any seismic damage. Therefore, the antiseismic performance of this construction stage is excellent. For the middle cantilever construction stage and the long cantilever construction stage, the exceedance probabilities are similar, and the exceedance probabilities of the slight, moderate, extensive, and collapse damage states are about 80%, 79%, 60%, and 55%, respectively. This means that under the action of strong earthquakes, a bridge at the middle cantilever construction stage and the long cantilever construction stage usually suffers from seismic damage. For the middle span closure

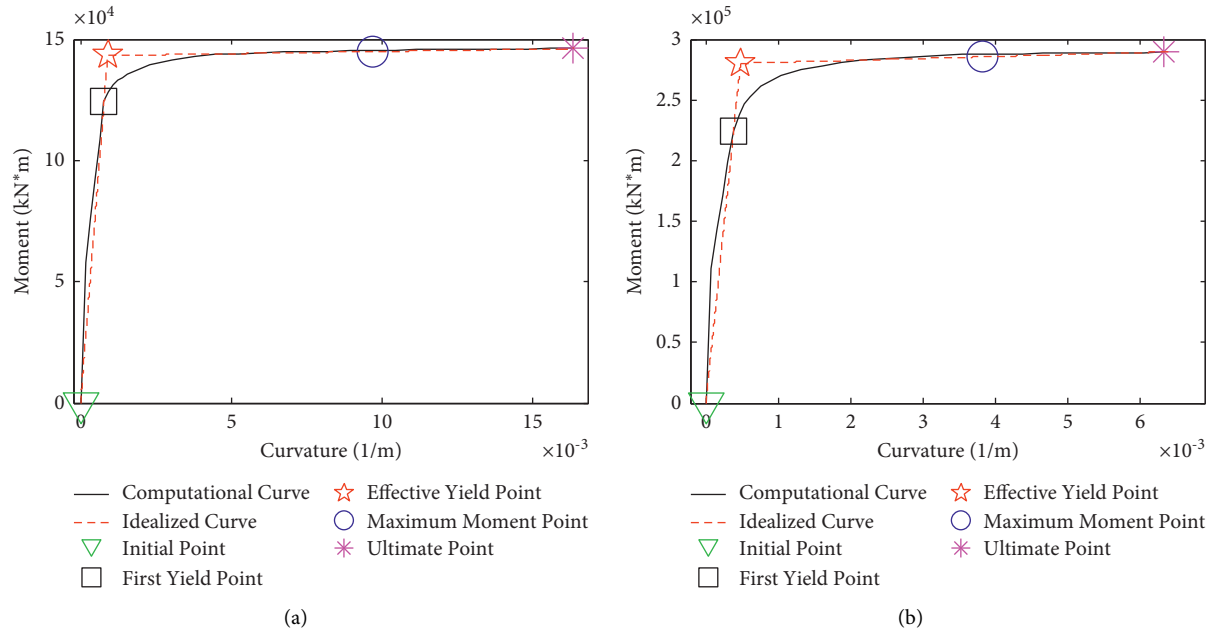

Figure 6: Moment-curvature relationships of middle pier bottom section (bridge completion stage). (a) Longitudinal moment-curvature relationships. (b) Transversal moment-curvature relationships.

Table 4: Damage evaluation indexes boundary values of the middle pier bottom (bridge completion stage).

Direction	Index	Unit	Slight damage	Moderate damage	Extensive damage	Collapse damage
Longitudinal	Curvature	1/m	7.82×10^{-4}	9.01×10^{-4}	9.70×10^{-3}	1.64×10^{-2}
	Moment	kN × m	1.24×10^{5}	1.43×10^{5}	1.45×10^{5}	1.46×10^{5}
Transversal	Curvature	1/m	3.84×10^{-4}	4.79×10^{-4}	3.59×10^{-3}	6.42×10^{-3}
	Moment	kN × m	2.25×10^{5}	2.80×10^{5}	2.85×10^{5}	2.90×10^{5}

Table 5: IDA results of the middle pier bottom (bridge completion stage).

Earthquake no.	PGA (g)	Transversal maximum moment (kN × m)	Longitudinal maximum moment (kN × m)
1	0.1	124715.30	41350.43
	0.2	249430.61	82700.87
	0.4	284632.28	143498.30
	0.8	295975.51	144432.25
	1.0	297487.94	144594.96
2	0.1	11055.41	9510.73
	0.2	22110.81	19021.46
	0.4	44221.62	38042.91
	0.8	88443.24	76085.82
	1.0	110554.06	95107.28
3	0.1	95882.67	116589.76
	0.2	191765.56	143736.31
	0.4	295770.93	144428.37
	0.8	303330.19	146002.37
	1.0	305830.99	147366.54
4	0.1	66169.98	43928.98
	0.2	132339.97	87857.97
	0.4	264679.60	143438.19
	0.8	293742.85	143818.36
	1.0	298630.06	144124.19

Table 5: Continued.

Earthquake no.	PGA (g)	Transversal maximum moment (kN × m)	Longitudinal maximum moment (kN × m)
5	0.1	111156.75	29670.38
	0.2	222313.50	59340.75
	0.4	286419.06	118682.54
	0.8	292862.12	144810.86
	1.0	297130.57	146277.70
6	0.1	93010.80	51934.77
	0.2	186021.60	103869.54
	0.4	284940.70	144977.70
	0.8	300716.87	149089.16
	1.0	303597.27	149702.63
7	0.1	93769.84	38333.40
	0.2	187539.68	76666.81
	0.4	284832.89	143386.89
	0.8	298734.72	145034.92
	1.0	302025.42	145959.40
8	0.1	104805.70	63977.45
	0.2	209611.40	127954.78
	0.4	286336.05	144716.45
	0.8	299258.12	146852.25
	1.0	301826.16	148718.42
9	0.1	76552.32	43323.90
	0.2	153104.64	86647.80
	0.4	281042.53	143559.38
	0.8	290690.42	144939.87
	1.0	294659.85	145455.57
10	0.1	138362.57	51103.98
	0.2	276725.15	102207.95
	0.4	292900.51	143900.92
	0.8	304259.53	147797.69
	1.0	307890.01	148617.52
11	0.1	85445.93	12397.04
	0.2	170891.86	24794.08
	0.4	283817.09	49588.17
	0.8	297073.82	99176.34
	1.0	297865.37	123970.42
12	0.1	83037.47	21897.19
	0.2	166074.93	43794.39
	0.4	283211.00	87588.77
	0.8	299157.07	143589.67
	1.0	300885.15	143720.47
13	0.1	66182.85	12746.55
	0.2	132365.70	25493.10
	0.4	264731.41	50986.20
	0.8	290176.33	101972.40
	1.0	297831.41	127465.51
14	0.1	29031.62	13745.21
	0.2	58063.24	27490.41
	0.4	116126.48	54980.83
	0.8	232252.97	109961.65
	1.0	280726.63	137451.98
15	0.1	24994.13	11864.14
	0.2	49988.26	23728.28
	0.4	99976.51	47456.56
	0.8	199953.03	94913.13
	1.0	249941.28	118641.41

Table 5: Continued.

Earthquake no.	PGA (g)	Transversal maximum moment (kN × m)	Longitudinal maximum moment (kN × m)
16	0.1	95988.89	93153.59
	0.2	191977.95	143593.86
	0.4	291159.88	152178.75
	0.8	341519.75	163385.42
	1.0	377424.26	168383.61
17	0.1	86019.30	54731.88
	0.2	172038.59	109463.75
	0.4	284273.13	146056.75
	0.8	303447.56	152343.62
	1.0	311396.04	155236.52
18	0.1	81512.48	80920.30
	0.2	163024.96	143487.87
	0.4	282744.71	152948.93
	0.8	318259.65	162343.61
	1.0	340261.62	165587.19
19	0.1	55297.90	71379.22
	0.2	110595.79	143302.00
	0.4	221193.84	148759.48
	0.8	306720.64	161842.72
	1.0	320054.15	169186.21
20	0.1	98706.94	70372.86
	0.2	197413.89	140745.71
	0.4	284130.64	145358.69
	0.8	305035.48	150225.29
	1.0	314483.53	151202.57

Table 6: Coefficients and standard deviations in the linear function fitting process.

Damage state	Parameter	Substructure	Middle cantilever	Long cantilever	Middle span closure	Bridge completion
Slight damage	A	1.000	3.313	3.438	2.827	2.959
	B	−0.329	6.523	6.383	8.066	8.158
	SD	0.900	3.595	3.589	3.321	3.393
Moderate damage	A	1.000	3.313	3.438	2.827	2.959
	B	−0.619	6.278	6.152	7.838	7.937
	SD	0.900	3.595	3.589	3.321	3.393
Extensive damage	A	1.000	3.313	3.438	2.827	2.959
	B	−3.146	3.973	3.955	5.673	5.922
	SD	0.900	3.595	3.589	3.321	3.393
Collapse damage	A	1.000	3.313	3.438	2.827	2.959
	B	−3.777	3.448	3.439	5.161	5.342
	SD	0.900	3.595	3.589	3.321	3.393

construction stage and the bridge completion construction stage, the exceedance probabilities are nearly the same, and the exceedance probabilities of slight, moderate, extensive, and collapse damage states are about 98%, 97%, 82%, and 78%, respectively. This means that under the action of strong earthquakes, a bridge at the middle span closure construction stage or the bridge completion construction stage always suffers from seismic damage, and it can easily suffer from extensive damage or collapse damage.

4.4. Seismic Damage Occurrence Probability. In Figure 7, the fragility represents the exceedance probability of a damage state, and it is the accumulated result of the occurrence probability of the damage state. Hence, the probabilities of occurrence of different damage states are

$$\begin{cases} p_1 = 1 - p_{f1} \\ p_2 = p_{f1} - p_{f2} \\ p_3 = p_{f2} - p_{f3}, \\ p_4 = p_{f4} - p_{f3} \\ p_5 = p_{f4} \end{cases} \tag{5}$$

where p_1, p_2, p_3, p_4, and p_5 are the occurrence probabilities of the no damage state, slight damage state, moderate damage state, extensive damage state, and collapse damage state and p_{f1}, p_{f2}, p_{f3}, and p_{f4} are the exceedance probabilities of the slight damage state, moderate damage state, extensive damage state, and collapse damage state, respectively. The occurrence probability curves of different states are shown in Figure 8.

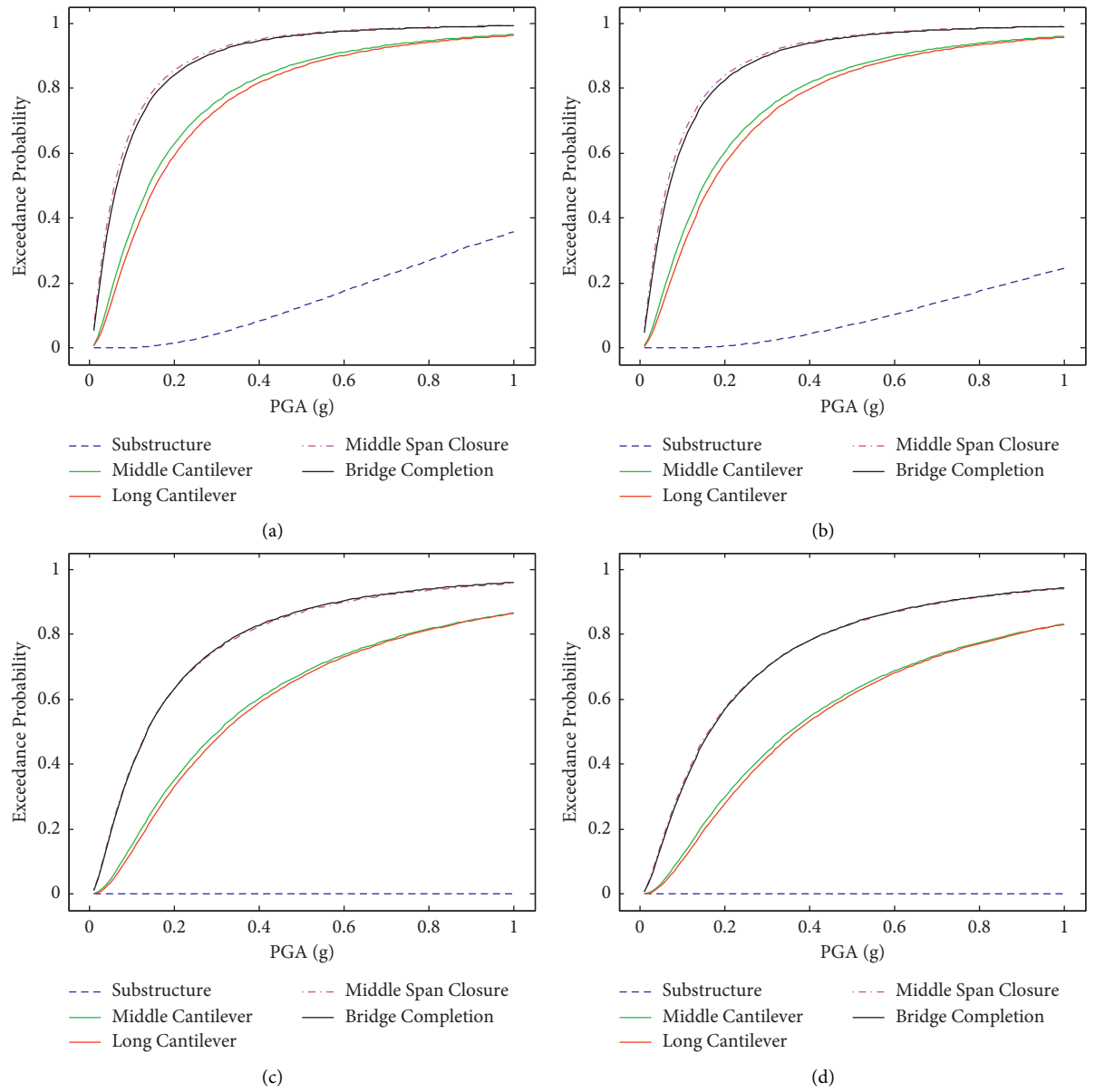

Figure 7: Fragility curves of different damage states. Exceedance probability of (a) slight damage state, (b) moderate damage state, (c) extensive damage state, and (d) collapse damage state.

Figure 8 shows that for different construction stages with different seismic intensities, the occurrence probabilities of the slight damage state and the extensive damage state are less than 12%, and the occurrence probabilities are low. This means that for the action of strong earthquakes, a bridge seldom suffers from extensive seismic damage or slight seismic damage. For different construction stages with different seismic intensities, the occurrence probabilities of the no damage state, moderate damage state, and collapse damage state are different, and the vulnerability evaluation and seismic defensive measurements should be conducted separately.

4.5. Seismic Mean Loss Ratio. The seismic loss ratio is the ratio of the lost value in an earthquake to the original value before an earthquake, the scope of which is 0 to 1. The mean loss ratio (MLR) is the mean value of the loss ratios. Based on the Pacific Earthquake Engineering Research Center (PEER) damage evaluation equation [17, 21], the bridge seismic mean loss ratio [22] is

$$\mathrm{MLR} = \sum_{j=1}^{k} \left(\frac{C_{s,j}}{I_s} * p_j \right), \tag{6}$$

where j is the damage state; k is the damage states total amount; $C_{s,j}$ is the recovery cost for damage state j; I_s is the replacement cost; $C_{s,j}/I_s$ is the loss ratio, which is the ratio of the recovery cost to the replacement cost; and p_j is the occurrence probability of damage state j.

In reference [22], the loss ratios of slight damage, moderate damage, and extensive damage for bridges are determined by their respective midvalues as 16%, 31%, and

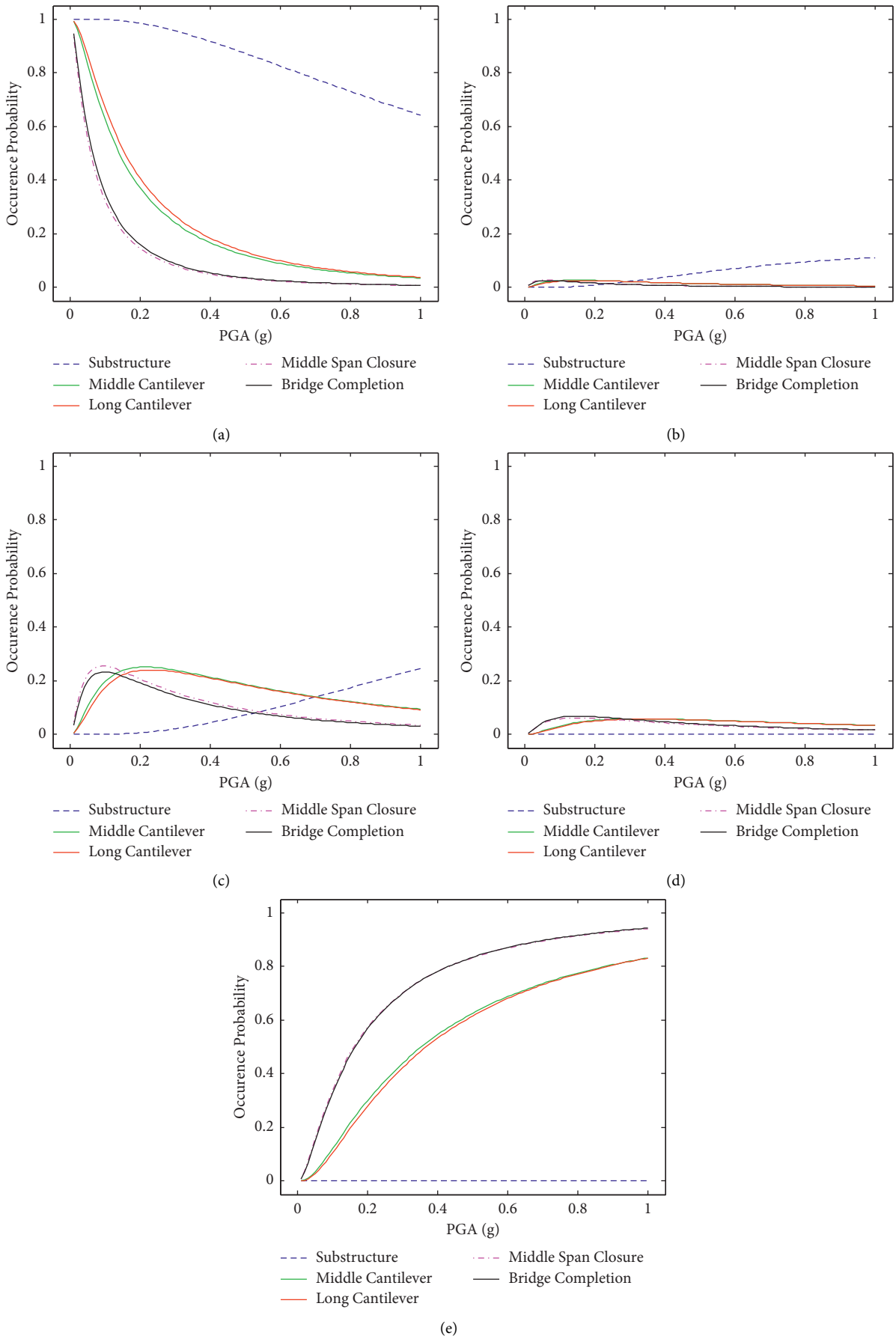

Figure 8: Occurrence probability curves of different damage states. Occurrence probability of (a) no damage state, (b) slight damage state, (c) moderate damage state, (d) extensive damage state, and (e) collapse damage state.

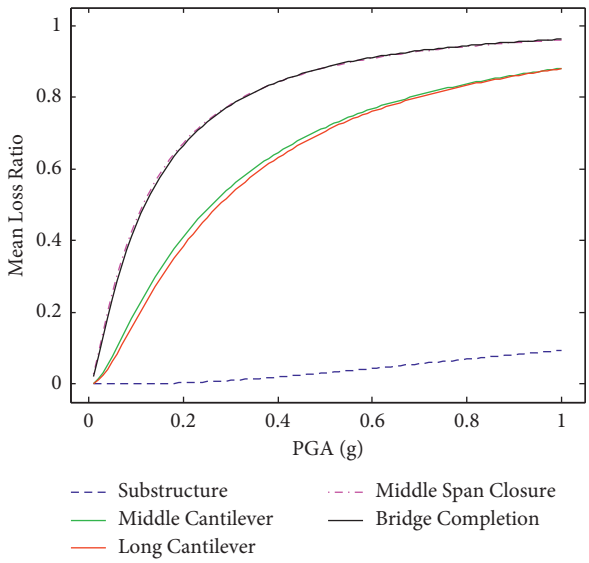

Figure 9: Seismic mean loss ratio curves of different construction stages.

56%. The loss ratios of no damage and collapse damage are 0% and 100%. Based on equation (6), the seismic mean loss ratios at different construction stages and for different PGAs can be determined. The seismic mean loss ratio curves of different construction stages are shown in Figure 9.

Figure 9 shows that the mean loss ratio curves of different construction stages are different. For the working condition of seismic PGA of 0.4 g, the conclusions can be acquired as follows. For the substructure construction stage, the mean loss ratio is about 5%. This means that under the action of strong earthquakes, a bridge at the substructure construction stage may only lose a small value. For the middle cantilever construction stage and the long cantilever construction stage, the mean loss ratios are similar, at about 65%. This means that under the action of strong earthquakes, a bridge at the middle cantilever construction stage and the long cantilever construction stage can lose more than half of the value. For the middle span closure construction stage and the bridge completion construction stage, the mean loss ratios are nearly the same, at about 85%. This means that under the action of strong earthquakes, a bridge at the middle span closure construction stage and the bridge completion construction stage may suffer from serious losses.

In addition, the plots shown in Figures 7 and 9 indicate that the seismic behavior of the bridge for middle cantilever and long cantilever construction stages are always similar, and for middle span closure and bridge competition, construction stages are practically the same. The reason is that the structural mechanical system for the middle cantilever and long cantilever construction stages are the same and so is the middle span closure and bridge competition construction stages. The structural mechanical system condition could also determine the structural mode shapes. As shown in Figure 2, the first and second mode shapes of the middle cantilever and long cantilever construction stages are the same, but the first and second modal frequencies are different. The first and second mode shapes of the middle span closure and bridge competition construction stages are the same. It can be summarized that the exceedance probability and mean loss rate are mainly determined by the structural mechanical system condition and the mode shapes but not the modal frequency.

5. Conclusions

In this study, the seismic vulnerability evaluation method of bridges under construction is proposed. Based on the case of a continuous girder bridge with the cast-in-place cantilever construction method, the seismic vulnerability evaluations of bridges at different construction stages are comparatively researched, and the conclusions are as follows:

(1) With the increase of the PGA, the system fragility and the mean loss ratio will increase.

(2) The fragility and vulnerability are mainly determined by the structural mechanical system condition and the mode shapes but not the modal frequency.

(3) For the bridge at the substructure construction stage, the seismic safety redundancy is large, and the seismic mean loss ratio is low. The bridge at the middle span closure construction stage or the bridge completion construction stage during strong earthquakes may suffer a serious loss, so many more seismic defensive measurements should be taken, and it is important to buy seismic insurance to transfer the possible seismic loss risk at these risky construction stages. For the bridge at the long cantilever construction stage or the middle cantilever construction stage, the seismic loss is moderate between the substructure construction stage and the cantilever construction stage.

(4) For the continuous girder bridges with the cast-in-place cantilever construction method, the mechanical system and characteristics, fragilities, and vulnerability of bridges at different construction stages are vastly different. Under the action of strong earthquakes, the vulnerability evaluation of bridges under construction should be conducted separately for different construction stages. Additionally, the seismic loss defensive measures for different construction stages should also be prepared differently.

Therefore, the research on the vulnerability evaluations for bridges at different construction stages under the action of strong earthquakes is useful. The research results can be applied to the evaluation of seismic risk occurrence probability and seismic loss ratio for the seismic insurance companies.

In addition, in future research, the aftershocks can also be considered by means of lengthening the ground motion records. The bridges under construction with the other construction methods can be researched with the construction stages vulnerability evaluation process proposed in this study. The influence of the bridge importance on the risk during the

construction stages can be further considered and discussed to make the research deeper and more comprehensive.

Data Availability

The data supporting the conclusion of the article are shown in the relevant figures and tables in the article.

Conflicts of Interest

The authors declare that there are no conflicts of interest regarding the publication of this article.

Acknowledgments

This work was financially supported by the National Key R&D Program of China (Grant no. 2018YFC1504602) and Scientific Research Fund of Institute of Engineering Mechanics, China Earthquake Administration (Grant no. 2018A02), and the support is greatly appreciated.

References

[1] W. B. Peng, J. D. Shen, X. Tang et al., "Review, analysis, and insights on recent typical bridge accidents," *China Journal of Highway and Transport*, vol. 32, no. 12, pp. 132–144, 2019.

[2] H. X. He, Y. F. Hu, and S. Wu, "Evaluation of structural vulnerability and resilience based on energy dissipation difference index and SIR model," *China Civil Engineering Journal*, vol. 53, no. 4, pp. 11–22, 2020.

[3] H. N. Li, H. Chen, and D. S. Wang, "A review of advances in seismic fragility research on bridge structures," *Engineering Mechanics*, vol. 35, no. 9, pp. 1–16, 2018.

[4] W. P. Wu, L. F. Li, S. C. Hu et al., "Research review and future prospect of the seismic fragility analysis for the highway bridges," *Earthquake Engineering and Engineering Dynamics*, vol. 37, no. 4, pp. 85–96, 2017.

[5] G. Lu, K. Wang, and W. Qiu, "Fragility-based improvement of system seismic performance for long-span suspension bridges," *Advances in Civil Engineering*, vol. 2020, pp. 1–21, Article ID 8693729, 2020.

[6] F. Wu, J. Luo, W. Zheng et al., "Performance-based seismic fragility and residual seismic resistance study of a long-span suspension bridge," *Advances in Civil Engineering*, vol. 2020, pp. 1–16, Article ID 8822955, 2020.

[7] J. Zhang and Y. Huo, "Evaluating effectiveness and optimum design of isolation devices for highway bridges using the fragility function method," *Engineering Structures*, vol. 31, no. 8, pp. 1648–1660, 2009.

[8] Y. Pan, A. K. Agrawal, and M. Ghosn, "Seismic fragility of continuous steel highway bridges in New York state," *Journal of Bridge Engineering*, vol. 12, no. 6, pp. 689–699, 2007.

[9] Y. Cao, Y. Liang, C. Huai, J. Yang, and R. Mao, "Seismic fragility analysis of multispan continuous girder bridges with varying pier heights considering their bond-slip behavior," *Advances in Civil Engineering*, vol. 2020, pp. 1–12, Article ID 8869921, 2020.

[10] C. Yang, W. L. Chen, and F. Teng, "The vulnerability analysis of bridge construction in aftershock area," *Engineering Mechanics*, vol. 33, pp. 251–256, 2016.

[11] R. Ohashi and O. Kiyomiya, "Examination of safety against earthquake at each stage of construction of long cable-stayed bridge," *Abstracts of Annual Meeting of JSCE*, vol. I, no. 531, 2016.

[12] W.-K. Hsu, W.-L. Chiang, Q. Xue et al., "A probabilistic approach for earthquake risk assessment based on an engineering insurance portfolio," *Natural Hazards*, vol. 65, no. 3, pp. 1559–1571, 2013.

[13] K. Porter, *Beginner's Guide to Fragility, Vulnerability, and Risk*, Springer Berlin Heidelberg, Berlin/Heidelberg, Germany, 2015.

[14] GB/T18208.4-2011, *Post-earthquake Field Works-Ppart 4: Assessment of Direct Loss*China Standard Press, Beijing, China, 2011.

[15] GB18306-2015, *Seismic Ground Motion Parameters Zonation Map of China*China Standard Press, Beijing, China, 2015.

[16] JTG/T2231-01-2020, *Specifications for Seismic Design of Highway Bridges*China Communications Press, Beijing, China, 2020.

[17] J. Liu, L. Zhang, H. Zhang, and T. Liu, "Seismic vulnerability analysis of single-story reinforced concrete industrial buildings with seismic fortification," *Structural Durability & Health Monitoring*, vol. 13, no. 2, pp. 123–142, 2019.

[18] A. Karamlou and P. Bocchini, "Functionality-fragility surfaces," *Earthquake Engineering & Structural Dynamics*, vol. 46, no. 10, pp. 1687–1709, 2017.

[19] M. J. N. Priestley and R. Park, "Strength and ductility of concrete bridge columns under seismic loading," *ACI Structural Journal*, vol. 84, no. S8, pp. 61–76, 1987.

[20] R. D. Zhao, Z. Q. Xu, J. B. Zou et al., "Seismic response analysis and performance evaluation of long-span cable-stayed bridge based on ANSYS," *Journal of Architecture and Civil Engineering*, vol. 35, no. 4, pp. 19–26, 2018.

[21] A. Karamlou, *Multi-scale Methodologies for Probabilistic Resilience Assessment and Enhancement of Bridges and Transportation Systems*, Ph. D. thesis, Lehigh University, Bethlehem, the USA, 2017.

[22] G. P. Cimellaro, A. M. Reinhorn, and M. Bruneau, "Framework for analytical quantification of disaster resilience," *Engineering Structures*, vol. 32, no. 11, pp. 3639–3649, 2010.